A GENERALIZED TRANSFER FUNCTION FOR THE
SEMICIRCULAR CANALS

Jack F. Landolt, Ph.D.
Head Biodynamics Section,
Defence and Civil Institute of
Environmental Medicine
Downsview, Ontario
CANADA M3M 3B9

and

Manning J. Correia, Ph.D.
Director of Research
Department of Otolaryngology
University of Texas Medical Branch
Galveston, Texas 77550
U.S.A.

DCIEM-80-P-09

SUMMARY

Steinhausen's hypothesis, that a simple torsion-pendulum model adequately describes the dynamics of semicircular-canal action, has received its share of criticism. This is primarily because of the fact that the time courses of afferent discharges and vestibular reactions to angular-acceleration stimuli only approximately relate to the time course obtained as a solution to the torsion-pendulum model for the same angular accelerations. Thus, there is a need to determine a generalized transfer function which delineates those components that provide meaning to Steinhausen's hypothesis from those which describe other phenomena such as "adaptation".

INTRODUCTION

Rotational head movements stimulate the sensory end organs of the semicircular canals of the inner ear, causing compensatory eye movements (nystagmus), appropriate to the plane of rotation, via a vestibulo-ocular reflex arc. However, the sensory epithelia of the semicircular canals, the cristae ampullares, are relatively inaccessible for direct functional study during normal physiological head movements. In the first place, they lie deep within the skull, enclosed by spongy and petrous bone and the osseous labyrinth. Secondly, any technique which exposes the hair cells or their nerve supply for neurobiological experimentation necessarily disrupts the vascular supply to the neuroepithelium and interferes with the ionic balance between the perilymph and endolymph. Thirdly, even when the membranous ampullae are exposed, it is difficult to perceive the extent to which the normally invisible cupula covers the crista and fills the ampulla of the duct. (It is the cupula which couples the mechanical energy of head motion to the receptor hair cells of the crista for transduction into neural impulses at the afferent terminals.) Thus, it is not surprising that, for over a century, the dynamic response characteristics of the semicircular canals have not been completely elucidated despite continuous investigation by many vestibular physiologists.

Historically, until the time of Fluorens (13), the semicircular canals were associated with the perception of sound. By sectioning the membranous semicircular canals in the pigeon and the rabbit, Fluorens established that eye, head, and body movements always occur in the same plane as that of the injured canal. Goltz (16), also investigating the pigeon, first associated these canals with bodily equilibrium. Breuer (5), Crum Brown (9), and Mach (26) suggested that the cristae ampullares respond to rotatory accelerations of the head. Moreover, they also hypothesized that the motion of the endolymph within the canal was responsible for eliciting the neural activity in the nerve endings (hydrodynamic theory). (Mach, however, later appears to have favoured a hydrostatic theory, i.e., that pressure is the adequate stimulus--see refs. 19, 28.) Ewald (11), using an "hydraulic hammer", produced artificial endolymphatic movements in the canals of pigeons and demonstrated that the direction of head nystagmus was dependent upon the direction of endolymph flow. Ewald's "law" was placed on a firmer footing when Lowenstein and Sand (25) established that the action-potential (impulse) frequency in fibers innervating the cristae varied according to the direction of angular movement of the head.

In order to describe the dynamics of the semicircular-canal system, Steinhausen (36, 37), and, subsequently, Egmond, Groen and Jonkees (10), proposed the so-called torsion-pendulum model. In this model, the instantaneous angular deflection of the cupula, $\xi(t)$, caused by an instantaneous angular acceleration of the head, $\alpha(t)$, is governed by the linear differential equation

$$\Theta \frac{d^2\xi(t)}{dt^2} + \Pi \frac{d\xi(t)}{dt} + \Delta\xi(t) = \Psi\Theta\alpha(t), \tag{1}$$

where Θ is the effective moment of inertia of the endolymph in the semicircular canal; Π is the viscous damping moment per unit angular velocity of endolymph relative to the wall of the membranous canal; Δ is the elastic-restoring moment per unit angular displacement of the endolymph relative to the membranous ampullary walls; and Ψ is a constant of proportionality relating ratio volumetric displacements (between the cupula and the canal endolymph). The transfer function of Eq. (1) can be written as:

_____
[1]DCIEM Publication 80-P-09

DISCLAIMER NOTICE

**THIS DOCUMENT IS BEST QUALITY
PRACTICABLE. THE COPY FURNISHED
TO DTIC CONTAINED A SIGNIFICANT
NUMBER OF PAGES WHICH DO NOT
REPRODUCE LEGIBLY.**

$$G_1(s) = \frac{\theta(s)}{A(s)} = \frac{1}{(\tau_1 s + 1)(\tau_2 s + 1)},$$

where $A(s)$ and $\theta(s)$ are Laplace transforms of $\alpha(t)$ and $\theta(t)$, respectively; $\theta = \Psi\tau_1\tau_2$; and $\tau_1 = \Pi/\Delta$ and $\tau_2 = \theta/\Pi$ are the so-called long and short time constants of the heavily-damped cupula/endolymph system (10, 20).

One way to test the adequacy of this model is to record the neural activity of the primary afferent fibers innervating the semicircular canals as they respond to appropriate stimulation. This has been done for a variety of species of animals (2, 3, 12, 17, 18, 23, 24, 33, 34, 35, 38) and the model has been found to be deficient. The present set of experiments was designed to study the mechanoneural response characteristics of primary afferent, semicircular-canal units in the pigeon, in order to determine whether or not a generalized transfer function could be obtained which would also describe similar neurodynamics in other species. (In testing to this model, the assumption is made that the afferent activity is proportional to the cupular displacement.)

METHODS

White King pigeons (Columba livia) were surgically prepared for microelectrode recording from peripheral units which innervated the semicircular canals (primarily, the anterior semicircular canal). The animal (with head immobilized) was oriented on board a rotatory device so that the center of its head plane was coincident with the plane of rotation (according to the type of canal being recorded from).

The main rotatory sequence consisted of a series of sinusoidal angular accelerations,

$$\alpha(t) = \alpha_m \sin 2\pi f t, \tag{3}$$

which were delivered to anesthetized preparations at frequencies, f, from 0.01 to 10 Hz with peak angular accelerations, α_m, of 2.0, 4.0, 8.0, 12.0, and 20.0 degrees/s^2 (t = real time in Eq. (3)). The single unit neural activity was amplified, displayed on an oscilloscope and recorded on magnetic tape according to conventional techniques. (One channel of the tape recorder was used for voice commentary; another for the stimulus reference signal.)

The stimulus reference signal was used to trigger a physiological signal analyzer (Nicolet Instruments Inc.) to count and store the taped, entrained action potentials in preselected appropriate time periods (bins) for up to 4096 sequential bins (see Fig. 1 for typical binned response). Fourier techniques were used on the binned neural data to obtain the magnitude of the peak amplitude of the response and the temporal (phase) relationship between the angular acceleratory stimulus and the fundamental component of the neural response.

Amplitude- and phase-values were used in a curve-fitting program on a PDP-11/40 minicomputer (Digital Equipment Corp.) to provide a distinct mathematical expression for the best-fitting transfer function for a linear system. (The steady-state frequency response for a linear system to a sinusoidal input angular acceleration may be found from gain,

$$|G(f)| = \{(\text{Re } G(f))^2 + (\text{Im } G(f))^2\}^{\frac{1}{2}}, \tag{4}$$

and phase,

$$\theta(f) = \tan^{-1} \{\text{Im } G(f)/\text{Re } G(f)\}, \tag{5}$$

spectra (Bode plots--see ref. 30), where Re $G(f)$ and Im $G(f)$ are the real and imaginary parts of $G(f)$, respectively.)

The method employs techniques in non-linear, least squares approximations and is applicable to both high- and low-order transfer functions (4). On the final interpolation in the program, the least squares error, LSE, of the best-fitting transfer function is obtained as

$$\text{LSE} = Y^T Y, \tag{6}$$

where Y is a residuals matrix (Y^T = transpose of Y) which is made up of error terms that express the differences between the experimental data and the model which is to be fitted. The mean square error,

$$\text{MSE} = \text{LSE}/(2L - S), \tag{7}$$

compares the goodness-of-fit of the derived transfer function to that of the experimental data ($2L$ = number of real and imaginary components of the data points, and S = number of parameters in the transfer function).

A more detailed description of the methodology may be found in a special monograph (7) and elsewhere (6, 21).

RESULTS AND DISCUSSION

The simplest transfer function that fitted the data for all units is of the form,

$$G'(s) = \frac{Cs^k}{(\tau_L s+1)} ,$$ (8)

where s^k is a fractional-order differential operator with $0 < k < 1$, and C is a gain constant with units in impulses^{-1}/degrees^{-1} (21). The Bode plots for four of the units are shown in Figs. 2-5, together with their best-fitting $G'(s)$, and the best-fitting torsion-pendulum model

$$G''(s) = \frac{C}{(\tau_L s+1)}.$$ (9)

(In Figs. 2-5, the effects of the $\tau_S = 2.0$ ms (vide infra) contributes no more than 1% to the gain spectra between $f = 0.01$ and 10 Hz; consequently, the single-pole transfer function, $G''(s)$, was an adequate representation of the torsion-pendulum model.) As is evident in the plots in Figs. 2-5, $G'(s)$ is a much better fit to the data than is $G''(s)$ (cf. the MSE values for the two models); and, in particular, the fit appears to improve with increasing k.

What, then, is the significance of k, or better still, s^k? Elsewhere, it is shown that

$$s^k = K \prod_{i=1}^{M} \left[\frac{D_i s (\zeta_{i-1} s+1)}{(\tau_i s+1)} \right],$$ (10)

where K and D_i are constants, $M = \infty$ (in theory, but finite when fitting Eq. (10) via a digital computer), and τ_i and ζ_{i-1} ($\zeta_0 = 0$) are time constants (21). Interestingly, when M = 1, Eq. (10) becomes

$$s^k = \frac{KD_1}{\tau_1} \left[\frac{\tau_1 s}{\tau_1 s+1} \right],$$ (11)

which has previously been defined as the transfer function of the adaptation operator (27, 40). Thus, s^k appears to be a form of adaptation. Work by Thorson and Biederman-Thorson (39) suggests that s^k represents a distributed relaxation process which is inherent in the sensory-adaptation mechanics of Limulus photoreceptors, vertebrate retinal receptors, chemoreceptors, and other mechanoreceptors. Investigations by Taglietti, Rossi and Casella (38) further suggest that s^k likely represents a relaxation phenomenon consisting of a time-varying intracellular electrogenic process, the components of which are summed with the generator potential in the receptor hair cell.

The coefficient of variation, CV, was determined as the ratio of the standard deviation of intervals to the mean interval, as obtained from interspike-interval distributions of spontaneous single unit activity. When a regression of CV on k was made for 28 units, a statistically-significant product-moment correlation ($r = 0.384$, $P < 0.05$) was obtained (21). Thus, the larger the CV is, the larger the value of k and, consequently, the amount of adaptation. Other work by Goldberg and Fernandez (15), in squirrel monkeys, shows that the CV is statistically correlated with semicircular-canal afferent fiber conduction rates. The thicker fibers have faster conduction rates and larger CVs. Together, these findings suggest that sensory adaptation phenomena are directly dependent on the innervation pattern of the afferent fibers.

The transfer function, $G'(s)$, differs also from that of $G''(s)$ in that τ_L is not single-valued as it is in the torsion-pendulum model; rather, it is unit dependent, taking on values from $\tau_L = 4.45$ to 22.17 s (mean $\pm$ SEM = 10.24 ± 1.20 s) (21). (In fitting Eq. (8), the coupling between k and τ_L would account for some of the five-fold range of values that were determined for τ_L. However, there is sufficient indication from other studies (30) that the response dynamics of small groups of contiguous hair cells are quite different from those of other groups.) Realizing that the hair-cell tufts are stiff (14), that their lengths vary according to their position on the sensory epithelium (crista) (22), that the number and thickness of the stereocilia can be variable (22), and that the mechanical properties of the cupula are not necessarily uniform across the crista (29), then it is plausible that τ_L could have a regional distribution.

The form

$$G(s) = \frac{Cs^k}{(\tau_L s+1)(\tau_S s+1)} ,$$ (12)

or sometimes,

$$G(s)(\tau_m s+1)$$ (13)

was fitted to published afferent-response data in the squirrel monkey (Saimiri sciureus) (12), the frog (Rana esculenta and R. temporaria)(3), the gerbil (Meriones unguiculatus) (35), and the guitarfish (Rhinobatos productus) (33). The parameter $\tau_m \equiv$ high frequency time constant which results from both the displacement and the rate of displacement of the cupula. Such a term has been obtained from analysis of vestibular-driven eye movements in man (Benson and Sternfeld, cited in ref. 1), and primary afferent canal responses in the squirrel monkey (12) and the elasmobranch fish (24). Table 1 lists k, τ_L, τ_S, and τ_m for these four species and for unit responses to white-noise stimuli obtained from pigeons that were primarily encéphale isolé preparations. For all species listed in Table 1, the MSE using Eqs. (12) or (13) was comparable to or smaller than that obtained with other models. Further details are given elsewhere (8).

TABLE 1: Parameters of a genera... ... ...nction (Eqs. (12) or (13)) describing semicircular-canal
dynamics in five sele...

Species	τ_1 (s)	τ_2 (ms)	τ_m (s)	Frequency range, f (Hz)
Squirrel monkey				
(a) "regular" unit	....	3	–	0.0125-8
(b) "irregular" unit	....	3	0.03	0.0125-8
Gerbil				
(a) CV ≤ 0.1	....	2	–	0.01-5
(b) CV > 0.1	....	2	–	0.01-5
Frog	....	–	–	0.0125-0.5
Guitarfish	....	–	–	0.02-4
Pigeon	....	2	–	0.5-16

In Table 1, the frequency ...
adequate value of τ_S. In genera...
from the biophysical propertie...
of the membranous vestibular a...
Money and colleagues (31) f r ...
($f = 1/2\pi\tau_S$) of 80 Hz in the me...
from canal afferents in the ...
given evidence that 5.70 ...
fitting to afferent data in the ...

... restricted in the frog and guitarfish to utilize an
... (= 0/Π) in the fits have been predetermined indirectly
...ymph and the dimensions of the pertinent anatomical features
... value τ_S = 2 ms, which was determined biophysically by
...gests that there should be an upper break frequency
...sponse dynamics in semicircular-canal afferents. Recording
...as frequency up to 70 Hz, Hartmann and Klinke (18) have
... in the same range as those determined empirically for
... 15).

REFERENCES

(1) BARNES, G.R. The Generat... ...ic Eye Movements in Vestibular Nystagmus. Rept. 529.
Farnborough, Hampshire: Roya' A... ...stitute of Aviation Medicine, 1973.

(2) BLANKS, R.H.I., ESTE., M... ...AM, .H. Physiologic characteristics of vestibular first-order
canal neurons in the cat. II. ...onstant angular accelerations. J. Neurophysiol. 38:
1250-1268, 1975.

(3) BLANKS, R.H.I. AND PRECH... ... ...al characterization of primary vestibular afferents in the
frog. Exp. Brain Res. 25: ...

(4) BRASSARD, J.R., CORREIA, M ...IT, J.P. A computer program for graphical and iterative
fitting of low and high orde... ... ...tions to biological data. Comp. Prog. Biomed. 4: 1-20, 1974.

(5) BREUER, J. Uber die Funk... ...gange des Ohrlabrinths. Wien. Med. Jahrb. 4: 72-124, 1874.

(6) CORREIA, M.J. AND LAN... ...aneous and driven responses from primary neurons of the
anterior semicircular cana ... ... Adv. Oto-Rhino-Laryngol. 19: 134-148, 1973.

(7) CORREIA, M.J., LAND... ... ...P.S., ANDERSON, P.J., AND LEE, M.A. Techniques for Prolonged
Single Unit Recording and ... ...Discharges from Primary Neurons in the Pigeon's Vestibular
Ganglion. Rept. 927. D w... ...nada: Defence and Civil Institute of Environmental Medicine,
1973.

(8) CORREIA, M.J., LAND... ... ..., EDEN, A.R., AND RAE, J.L. A species comparison of linear
and nonlinear transfer char... ... primary afferents innervating the semicircular canal. In:
Vestibular Function and M rp... ... by T. Gualtierotti. Heidelberg/New York: Springer (in press),
1980.

(9) CRUM BROWN, A. On the se ... ...tion and the anatomy and physiology of the semicircular canals
of the inner ear. J. Anat ... ... 7-421, 1874.

(10) EGMOND, A.A.J. VAN, ...NGREEN, L.B.W. The mechanics of the semicircular canal.
J. Physiol., London. 110: ...

(11) EWALD, J.R. Physi ... ...ungen ueber das Endorgan des Nervus octavus. Wiesbaden:
Bergmann, 1892.

(12) FERNANDEZ, C. AND GOLDBERG, J.M. Physiology of peripheral neurons innervating semicircular canals of the squirrel monkey. II. Response to sinusoidal stimulation and dynamics of peripheral vestibular system. J. Neurophysiol. 34: 661-675, 1971.

(13) FLOURENS, P. Recherches Expérimentales sur les Propriétés et les Fonctions du Système Nerveux dans les Animaux Vertébrés. Paris: Crevot, 1824.

(14) FLOCK, Å., FLOCK, B., AND MURRAY, E. Studies on the sensory hairs of receptor cells in the inner ear. Acta Oto-Laryngol. 83: 85-91, 1977.

(15) GOLDBERG, J.M. AND FERNANDEZ, C. Conduction times and background discharge of vestibular afferents. Brain Res. 122: 545-550, 1977.

(16) GOLTZ, F. Uber die physiologische Bedeutung der Bogengange des Ohr abyrinthes. Arch. Ges. Physiol. 3: 172-192, 1870.

(17) GROEN, J.J., LOWENSTEIN, O., AND VENDRIK, A.J.H. The mechanical analysis of the responses from the end-organs of the horizontal semicircular canal in the isolated elasmobranch labyrinth. J. Physiol., London. 117: 329-346, 1952.

(18) HARTMANN, R. AND KLINKE, R. System analysis of properties of primary afferent vestibular fibres from the horizontal semicircular canal in goldfish. In: IFAC-Symposium on Control Mechanisms in Bio- and Ecosystems, Vol. 3, Visual and Vestibular Control of Movements, Leipzig, D.D.R., 1977, p. 108-115.

(19) HENN, V. AND YOUNG, L.R. Ernst Mach on the vestibular organ 100 years ago. ORL 37: 138-148, 1975.

(20) JONES, G.M. AND MILSUM, J.H. Spatial and dynamic aspects of visual fixation. IEEE Trans. Bio-Med. Eng. 12: 54-62, 1965.

(21) LANDOLT, J.P. AND CORREIA, M.J. Neurodynamic response analysis of anterior semicircular canal afferents in the pigeon. J. Neurophysiol. (in press), 1980.

(22) LINDEMAN, H.H. Studies on the morphology of the sensory regions of the vestibular apparatus. Ergeb. Anat. 42: 1-113, 1969.

(23) LOUIE, A.W. AND KIMM, J. The response of 8th nerve fibers to horizontal sinusoidal oscillation in the alert monkey. Exp. Brain Res. 24: 447-457, 1976.

(24) LOWENSTEIN, O. AND COMPTON, G.T. A comparative study of the responses of isolated first-order semicircular canal afferents to angular and linear acceleration, analysed in the time and frequency domains. Proc. Roy. Soc., London, Ser. B. 202: 313-338, 1978.

(25) LOWENSTEIN, O., AND SAND, A. The activity of the horizontal semicircular canal of the dogfish, Scyllium canicula. J. Exp. Biol. 13: 416-428, 1936.

(26) MACH, E. Physikalishe Versuche uber den Gleichgewichtssinn des Menschen. Wien. Akad. Sitzungsberichte III. 69: 124-143, 1873.

(27) MALCOLM, R. AND MELVILL JONES, G.A. A quantitative study of vestibular adaptation in humans. Acta Oto-Laryngol. 70: 126-135, 1970.

(28) MAYNE, R. The dynamic characteristics of the semicircular canals. J. Comp. Physiol. Psychol. 43: 309-319, 1950.

(29) MCLAREN, J.W. The Configuration of Movement of the Semicircular Canal Cupula (Ph.D. Thesis). Iowa City: Univ. of Iowa, 1977.

(30) MILSUM, J.H. Biological Control System Analysis. New York: McGraw-Hill, 1966.

(31) MONEY, K.E., BONEN, L., BEATTY, J.D., KUEHN, L.A., SOKOLOFF, M. AND WEAVER, R.S. Physical properties of fluids and structures of vestibular apparatus of the pigeon. Am. J. Physiol. 220: 140-147, 1971.

(32) O'LEARY, D.P., DUNN, R.F., AND HONRUBIA, V. Functional and anatomical correlation of afferent responses from the isolated semicircular canal. Nature 251: 225-227, 1974.

(33) O'LEARY, D.P. AND HONRUBIA, V. Analysis of afferent responses from isolated semicircular canal of guitarfish using rotational acceleration white-noise inputs. II. Estimation of linear system parameters and gain and phase spectra. J. Neurophysiol. 39: 645-659, 1976.

(34) PETERKA, R.J., O'LEARY, D.P., AND TOMKO, V.L. Linear system techniques for the evaluation of semicircular canal afferent responses using white noise rotational stimuli. In: Vestibular Mechanisms in Health and Disease, edited by J.D. Hood. London/New York: Academic, 1978, p. 10-17.

(35) SCHNEIDER, L.W. AND ANDERSON, D.J. Transfer characteristics of first and second order lateral canal vestibular neurons in gerbil. Brain Res. 112: 61-76, 1976.

(36) STEINHAUSEN, W. Uber den Nachweis der Bewegung der Cupula in der intaken Bogengangsampulle des Labyrinthes bei der naturlichen rotatorischeu and calorischen Reizung. Arch. Ges. Physiol. 228: 322-328, 1931.

(37) STEINHAUSEN, W. Uber die Beobachtung der Cupula in den Bogengansampullen des Labyrinths des lebenden Hechts. Arch. Ges. Physiol. 230: 500-512, 1934.

(38) TAGLIETTI, V., ROSSI, M.L., AND CASELLA, C. Adaptive distortions in the generator potential of semicircular canal sensory afferents. Brain Res. 123: 41-57, 1977.

(39) THORSON, J. AND BIEDERMAN-THORSON, M. Distributed relaxation processes in sensory adaptation. Science 183: 161-172, 1974.

(40) YOUNG, L.R. AND OMAN, C.M. Model of vestibular adaptation to horizontal rotations. Aerospace Med. 40: 1076-1080, 1969.
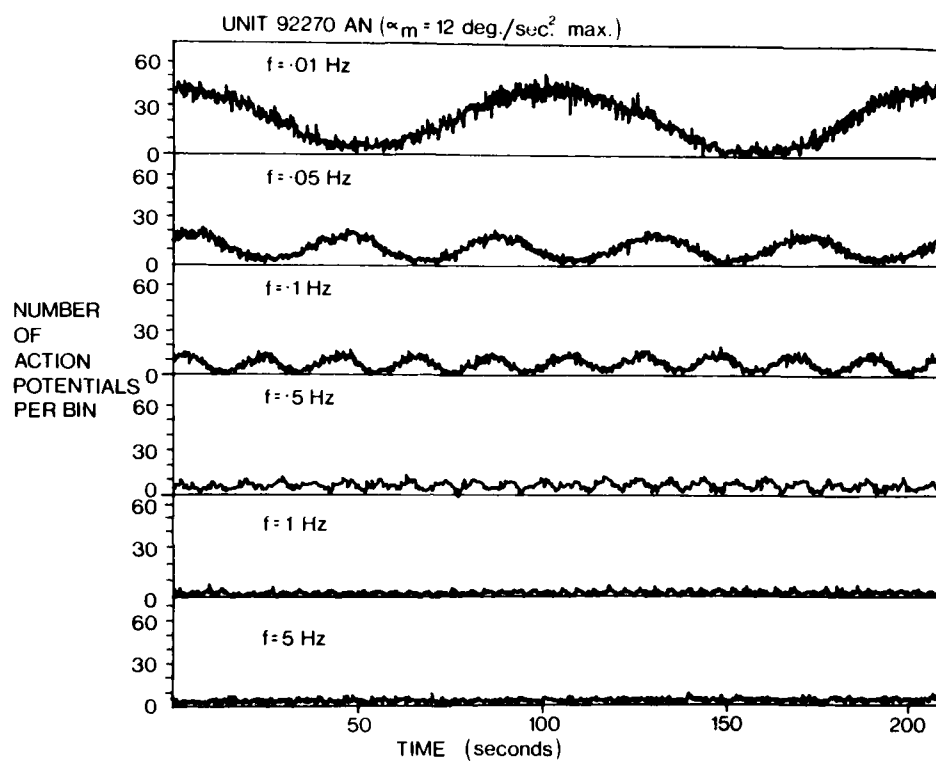
Fig. 1. Typical binned neural response. Bin widths are 0.2 (for f = 0.01 Hz), 0.1 (for f = 0.05 to 0.5 Hz), 0.05 (for f = 1.0 Hz), and 0.01 s (for f = 5 Hz).
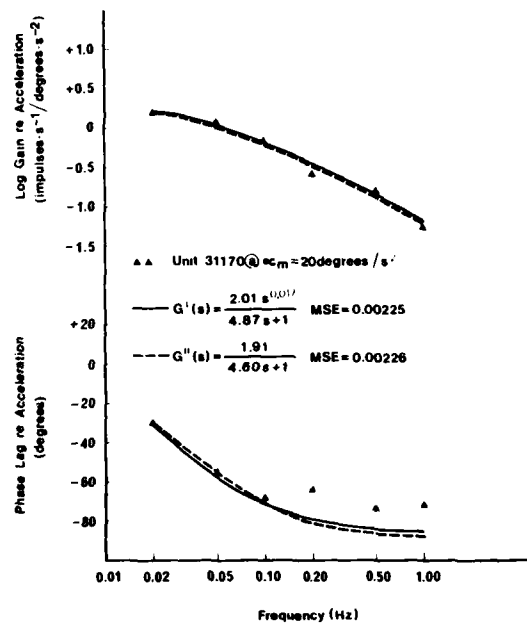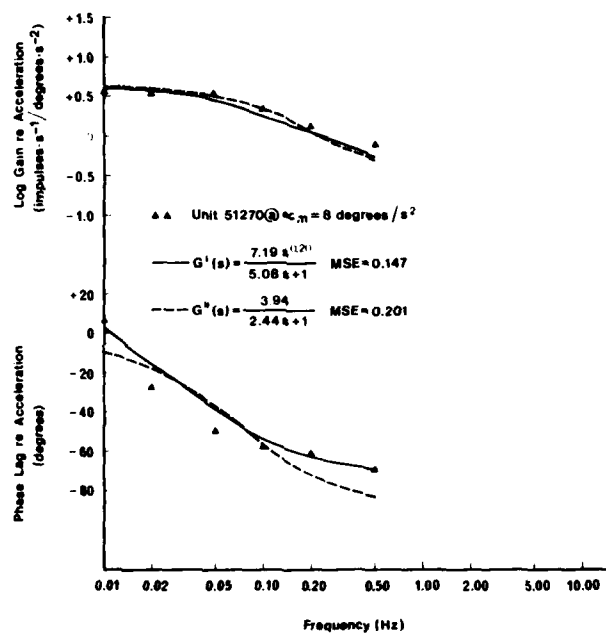
B10-8

Fig. 2.   Bode plot of Unit 31170 re angular acceleration and fits of models to data.

Fig. 4.   Bode plot of Unit 51270 re angular acceleration and fits of models to data.
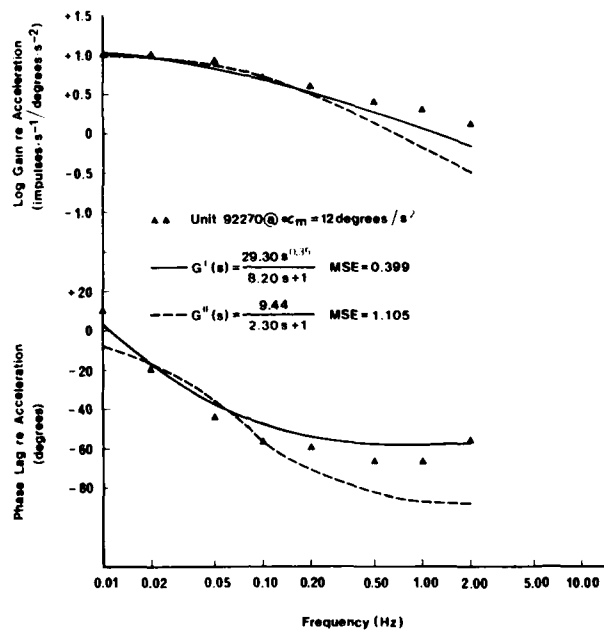
Log Gain re Acceleration (impulses·s^{-1}/degrees·s^{-2})

+1.5
+1.0
+0.5
0
-0.5
-1.0

▲ ▲   Unit 92270 @ αc_m = 12 degrees / s^2

—— $G'(s) = \dfrac{29.30\, s^{0.35}}{8.20\, s + 1}$ MSE = 0.399

---- $G''(s) = \dfrac{9.44}{2.30\, s + 1}$ MSE = 1.105

Phase Lag re Acceleration (degrees)

+20
0
-20
-40
-60
-80

0.01 0.02 0.05 0.10 0.20 0.50 1.00 2.00 5.00 10.00

Frequency (Hz)

Fig. 4.   Bode plot of Unit 92270 re angular acceleration and fits of models to data.

Log Gain re Acceleration (impulses·s^{-1}/degrees·s^{-2})

+1.5
+1.0
+0.5
0
-0.5
-1.0

▲ ▲   Unit 102269 @ αc_m = 12 degrees / s^2

—— $G'(s) = \dfrac{66.94\, s^{0.57}}{22.17\, s + 1}$ MSE = 0.192

---- $G''(s) = \dfrac{6.88}{1.77\, s + 1}$ MSE = 0.538

Phase Lag re Acceleration (degrees)

+20
0
-20
-40
-60
-80

0.01 0.02 0.05 0.10 0.20 0.50 1.00 2.00 5.00 10.00
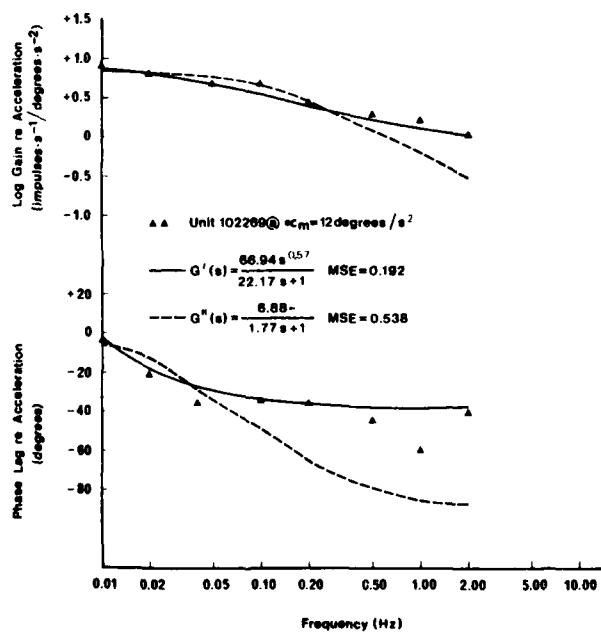
Frequency (Hz)

Fig. 5.   Bode plot of Unit 102269 re angular acceleration and fits of models to data.

ATE
LMED
8